Adsorption and Quantum Chemical Studies on Piperidin-4-One Derivatives for the Corrosion of Mild Steel in 1 M HCl Medium

Kalaiselvi K and Kavithamani A
Department of Chemitry, P.S.G.R.krishnammal College for Women, Coimbatore-641 004, INDIA

Abstract

The inhibition performance of synthesized 3-ethyl-2,6-biquinonyl-piperidin-4-one (CQEP) and 3-butyl-2,6-biquinonyl-piperidin-4-one (CQBP) were investigated as corrosion inhibitors for mild steel in a 1 M HCl solution using the weight loss, electrochemical polarization and electrochemical impedance spectroscopy (EIS) techniques. It was found that the inhibition efficiency of these inhibitors increased with increasing concentration. The effect of temperature (303, 313, 323 and 333 K) on the corrosion rate was investigated and some thermodynamic parameters (E_a, ΔH^o and ΔS^o) were calculated. Polarization studies showed that both inhibitors studied were of a mixed type in nature. The adsorption of inhibitors on the mild steel surface obeys the Langmuir adsorption isotherm. Scanning electron microscopy (SEM) and atomic adsorption spectroscopy (AAS) were performed for the surface study of the uninhibited and inhibited mild steel samples. Density functional theory (DFT) was employed for theoretical calculations. The theoretical results were found to be consistent with the experimental data reported.

Keywords: Inhibitors, adsorption, polarization, impedance, AAS, SEM, quantum studies.

Introduction

Corrosion of mild steel is an inevitable process that produces a deterioration of materials and their properties resulting in massive economic losses especially when it occurs in aggressive media like hydrochloric acid[1]. In view of the problems created by mild steel corrosion, several researches on the methods of inhibition of its corrosion have been reported and it has been established that the use of inhibitors is one of the best methods of the prevention of the corrosion of mild steel in acidic medium[2]. The study of corrosion processes and their inhibition by organic compounds is a very active field of research[3]. Over the years, considerable efforts have been deployed to find suitable corrosion inhibitors of organic origin in various corrosive media[4]. Most of the organic inhibitors containing nitrogen, oxygen, sulfur atoms and multiple bonds in their molecules facilitate adsorption on the metal surface[5,6]. Researchers conclude that the adsorption on the metal surface depends mainly on the physicochemical properties of the inhibitor, such as the functional group, molecular electronic structure, electron density at the donor atom, p orbital character and the molecular size[7]. The planarity and the lone electron pairs in the hetero atoms are important features that determine the adsorption of molecules on the metallic surface[8].

In the present work an attempt has been made to synthesize 3-ethyl-2,6-biquinonyl-piperidin-4-one (CQEP) and 3-butyl-2,6-biquinonyl-piperidin-4-one (CQBP) compounds as corrosion inhibitor for mild steel in 1 M HCl using weight loss, potetiodynamic polarization and electrochemical impedance spectroscopy (EIS). The adsorption natures of the inhibited and

uninhibited solutions are analyzed by using atomic absorption spectroscopy (AAS). The surface morphology of the mild steel was evaluated using SEM images. Quantum chemical calculations have been performed and several quantum chemical parameters were calculated and correlated with the corresponding inhibition efficiencies.

Material and Methods

Materials and Chemicals: Mild steel of size 3 cm x 1 cm x 0.5 cm are used, which consists of the following composition C, 0.051% Mn, 0.19% Si, 0.002% P, 0.018% S, 0.012% Cr, 0.019% Mo, 0.008% Ni, 0.031% and the reminder iron were used for weight loss and electrochemical measurements. The specimens were polished with 1/0, 2/0, 3/0 and 4/0 grades of emery sheets and degreased with acetone and dried using a drier. The plates were kept in a desiccator to avoid the absorption of moisture.

Synthesis of the inhibitor: Step 1: Synthesis of 2-Chloro-3-formyl quinoline: To a solution of acetanilide (5 mmoles) in dry DMF (15 mmoles) at 0-5[0]C temperature, Phosphoryl chloride (60 mmoles) was added dropwise with stirring and mixture was then stirred for 5 minutes and the resulting solid was filtered, washed well with distilled water and dried. The compound was recrystallised from ethyl acetate.

Step 2: Synthesis of 3-substituted-2,6-bisquinolinyl-piperidin-4-ones: A mixture of ketone (50 mmoles), ammonium acetate (50 mmoles) and 2-Chloro-3-formyl quinoline (100 mmoles) in glacial acetic acid were heated to

simmering carefully. It was kept at room temperature for 24 hours. To a viscous liquid obtained, ether (25 ml) was added, followed by concentrated hydrochloric acid (15 ml) and cooled in ice water. The precipitated hydrochloride was filtered and washed with ethanol-ether (1:5) mixture. The hydrochloride was suspended in acetone and made alkaline using ammonia solution. On dilution with excess of water, the base was precipitated, filtered, dried and recrytallised from ethanol.

Non-Electrochemical Techniques: Weight loss method: The initial weight of the polished mild steel plates were taken.1M
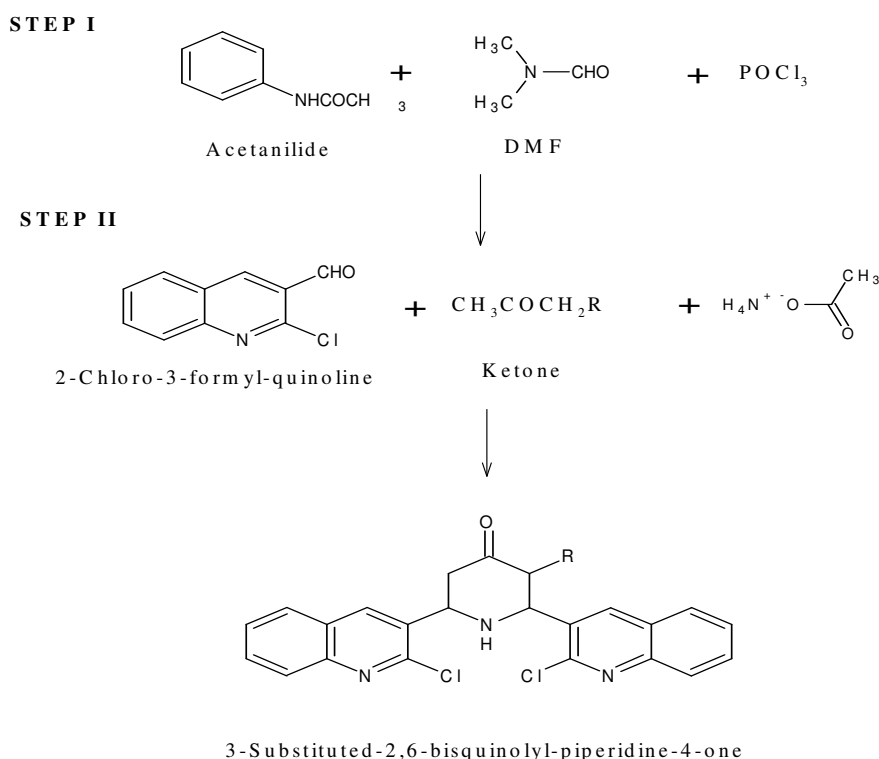
HCl was taken in an 100 ml beaker and the specimens were suspended in triplicates into the solution using glass hooks. Care was taken to ensure the complete immersion of the plates. After a period of 3 hours the plates were removed, washed with distilled water, dried and weighed. From the initial and final weight of the plates (i.e., before and after immersion in the solution) the loss in weight was calculated. The experiment was repeated for various inhibitor concentrations in 1M HCl. The inhibition efficiency, corrosion rate and surface coverage were calculated from the weight loss results using the formulas,
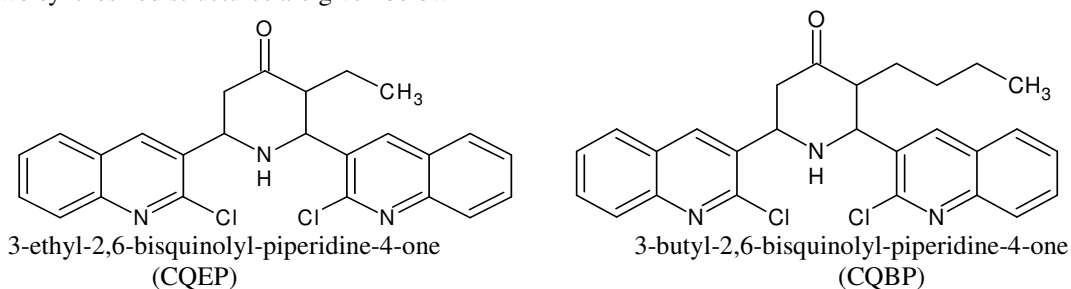
$$\text{Inhibition Efficiency (\%)} = \frac{\text{Weight Loss without Inhibitor} - \text{Weight Loss with Inhibitor}}{\text{Weight Loss without Inhibitor}} \times 100$$

$$\text{Corrosion Rate (mpy)} = \frac{534 \times \text{Weight Loss in mgs}}{\text{Density in g/cm3 X Area in sq.inch X Time in hours}}$$

$$\text{Surface Coverage } (\theta) = \frac{\text{Weight Loss without Inhibitor} - \text{Weight Loss with Inhibitor}}{\text{Weight Loss without Inhibitor}}$$

STEP I

Acetanilide + DMF + POCl$_3$

STEP II

2-Chloro-3-formyl-quinoline + CH$_3$COCH$_2$R + H$_4$N$^+$ $^-$O— (Ketone)

3-Substituted-2,6-bisquinolyl-piperidine-4-one

The following two synthesized structures are given below

3-ethyl-2,6-bisquinolyl-piperidine-4-one
(CQEP)

3-butyl-2,6-bisquinolyl-piperidine-4-one
(CQBP)

Scheme-1

To study the effect of temperature, the above procedure was carried out at different temperature range i.e., (313-333K) using thermostat with the inhibitor concentration of 0.1-0.5 mM. Activation energy (E_a), Free energy of adsorption (ΔG^0), Enthalpy and Entropy (ΔH^0 & ΔS^0) were calculated using the formula,

$$E_a = -2.303 \times 8.314 \times slope \ (KJ)$$

The free energy of adsorption ΔG^o_{ads} has been calculated from the equilibrium constant of adsorption using the equation

$$\Delta G = -RT \times 2.303 \times \log (55.5K)$$

Where: $K = \theta / C (1- \theta)$ Θ = Surface coverage of the inhibitor, C = Concentration of the inhibitor in mM/100ml, K = equilibrium constant, R = gas constant, T = Temperature.

Electro chemical studies: An electrochemical cell assembly of three electrodes was used for potentio dynamic polarization and electrochemical impedence measurements in which working electrode was mild steel, calomel electrode was the reference electrode and platinum wire was counter electrode. The electrochemical measurements were carried out in a glass cell with the capacity of 100 ml. The mild steel rod of size 0.6 mm was then placed in the test solution (uninhibited and inhibited solution) for 10- 15 minutes before electrochemical measurements. The electrochemical impedance spectroscopy (EIS) and Tafel polarization were conducted in a electrochemical measurements unit. The EIS measurement was made at corrotion potential over a frequency range of 1MHz to 10MHz with signal amplitude of 10mV. The Tafel polarization were made after EIS for a potential range of -200mV to + 200 mV with respect to open circuit potential, at a scan rate of 1mV/sec. From Nysquist plot (Z real Vs Z imaginary) electrochemical resistance (R_t) and double layer capacitance C_{dl} were calculated. From the plot of potential, E Vs log I, the corrosion potential E_{corr}, corrosion current, I_{corr} and Tafels slope for the cathodic and anodic reaction b_c and b_a were obtained.

Inhibitor efficiency by potentio dynamic polarization method: The inhibitor efficiency was calculated from the value of I_{corr} by using the formula

$$\text{Inhibition Efficiency (\%)} = \frac{I_{corr}(\text{blank}) - I_{corr}(\text{inh})}{I_{corr}(\text{blank})} \times 100$$

Where: I_{corr} (blank) = the corrosion current in the absence of the inhibitor. I_{corr} (inh) = the corrosion current in the presence of the inhibitor.

Inhibitor efficiency by AC impedance method: The inhibitor efficiency was calculated using the formula

$$\text{Inhibition Efficiency (\%)} = \frac{R_t(\text{inh}) - R_t(\text{blank})}{R_t(\text{inh})}$$

Where, R_t (inh) = the charge transfer resistance in the presence of the inhibitor. R_t (blank) = the charge transfer resistance in the absence of the inhibitor.

Scanning Electron Microscope (SEM): The specimens are exposed in 100 ml of 1 M HCl solution in absence and presence of inhibitor for 3 hours at room temperature and then washed with distilled water, after drying the specimens, they were examined for surface analysis by SEM. A scanning electron microscope (JEOL Model) was used to study the morphology of the mild surface in the absence and presence of the inhibitor.

Atomic Absorption Spectroscopy (AAS): Atomic Absorption Spectrophotometer (model GB 908/AUSTRALIA) was used for estimating the amount of dissolved iron in the corrodent solution containing various concentrations of polyamides in 1M H_2SO_4 after exposing the mild steel specimen for 3 hours. From the amount of dissolved iron, the inhibitor efficiency was calculated.

$$\text{Inhibition efficiency (\%)} = \frac{B-A}{B} \times 100$$

Where: B is the amount of dissolved iron in the absence of inhibitor, A is the amount of dissolved iron in the presence of inhibitor.

Quantum chemical calculations: The molecular structure of 3-ethyl-2,6-biquinonyl-piperidin-4-one (CQEP) and 3-butyl-2,6-biquinonyl-piperidin-4-one (CQBP) were drawn using the Chem Sketch. All the quantum calculations were performed with complete geometry optimization by using standard Gaussian 03 software. The guantum chemical parameter were calculated using the dencity functional theory (DFT) method at the level of B3LYP/6-31G (d,p). The following quantum chemical parameters were considered: the energies of highest occupied molecular orbital (E_{HOMO}) and the lowest unoccupied molecular orbital (E_{LUMO}), the energy gap (ΔE) between E_{HOMO} and E_{LUMO}, dipole moment (μ), ionization potential (I), electron affinity (A), absolute electronegativity (χ), global hardness (η), global electrophilicity index (ω) and softness (S).

Results and Discussion

Weight loss, corrosion rate and inhibition efficiency: The weight loss for the mild steel in 1 M HCl containing different concentrations of the 3-ethyl-2,6-biquinonyl-piperidin-4-one (CQEP) and 3-butyl-2,6-biquinonyl-piperidin-4-one (CQBP) compounds are presented in table-1. The weight loss with concentration of the inhibitor (CQEP and CQBP) is plotted graphically in the figure-1. It is clear that the weight loss decreases with increase in the inhibitor concentration, suggesting that the number of molecules adsorbed on the mild steel surface, locking the active sites from acid attack and thereby protecting the metal from corrosion.

Table-1
Inhibition efficiencies of mild steel at various concentrations of inhibitor (CQEP and CQBP) in 1 M HCl by weight loss measurement at room temperature

Name of the inhibitor	Inhibitor concentration (mM)	Weight loss (g)	Inhibition efficiency (%)	Corrosion rate (mpy)	Degree of Surface Coverage (θ)
CQEP	Blank	0.01095	-	215627.4	-
	0.1	0.00126	88.45	24811.92	0.8845
	0.3	0.00112	89.77	23630.40	0.8977
	0.5	0.00087	92.05	17132.04	0.9205
CQBP	Blank	0.01701	-	334960.9	-
	0.1	0.00169	90.37	33279.48	0.9037
	0.3	0.00101	94.30	19888.92	0.9430
	0.5	0.00064	96.23	12602.88	0.9623

The plot of corrosion rate with concentration is shown in the figure-3. From the figure-3 indicates the corrosion rate decreases with increase in inhibitor concentration. This implies that CQEP and CQBP act through adsorption on mild steel surface and formation of a barrier layer between the metal and the corrosive medium.

Inhibition efficiency increases with increase in the inhibitor (CQEP and CQBP) concentration (0.1, 0.3 and 0.5 mM) for mild steel. A plot of inhibition efficiency with concentration of the inhibitor (CQEP and CQBP) as shown in figure-2. This may be due to the adsorption of inhibitor (CQEP and CQBP) on metal surface through non-bonding electron pairs of nitrogen and oxygen atoms as well as the л-electrons of the aromatic rings. The high inhibitive performance of CQBP inhibitor compared to CQEP.
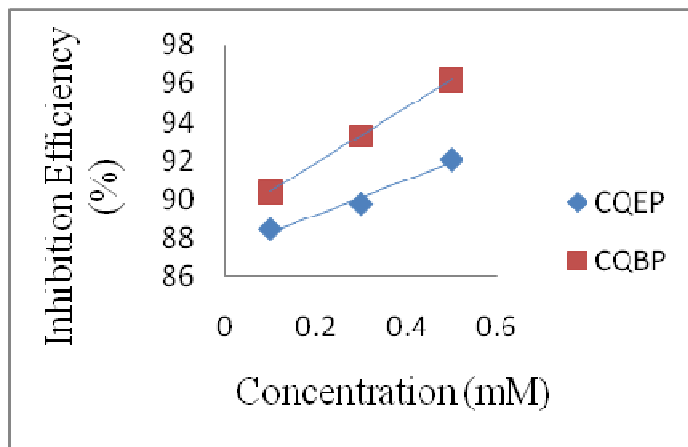
Figure-2
Effect of concentrations on the inhibition efficiency of inhibitor for mild steel in 1 M HCl
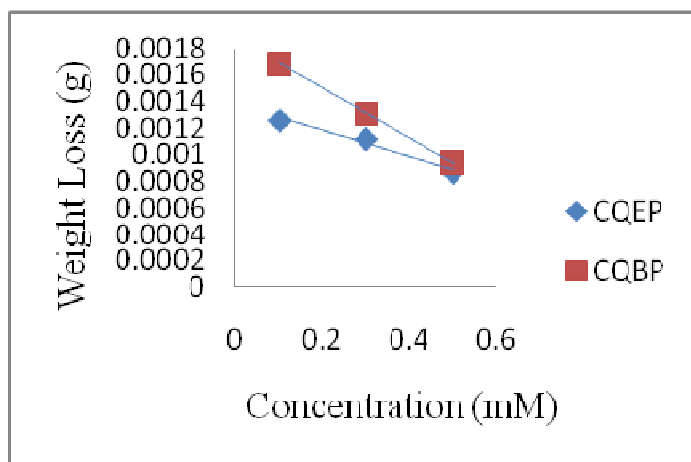
Figure-1
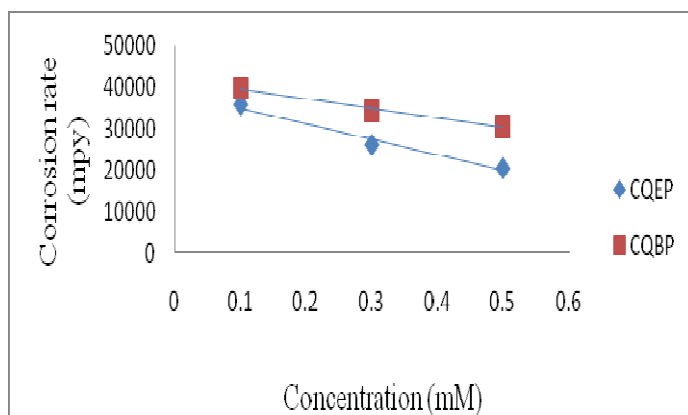**Effect concentrations on the weight loss of inhibitor for mild steel in 1MHCl**

Figure-3
Effect of concentrations on the corrosion rate of inhibitor for mild steel in 1 M HCl

Table-2
Inhibition efficiencies of mild steel at various concentrations of inhibitor (CQEP and CQBP) in 1 M HCl by weight loss measurement at higher temperature

Name of the inhibitor	Temperature (K)	Inhibitor concentration (mM)	Weight loss (g)	Inhibition efficiency (%)	Corrosion rate (mpy)	Degree of Surface Coverage (θ)
CQEP	303	Blank	0.01095	-	215627.4	-
		0.1	0.00126	88.45	24811.92	0.8845
		0.3	0.00112	89.77	23630.40	0.8977
		0.5	0.00087	92.05	17132.04	0.9205
	313	Blank	0.04158	-	818793.4	-
		0.1	0.00632	84.80	124453.4	0.8480
		0.3	0.00457	86.84	89992.44	0.8684
		0.5	0.00417	88.99	82115.64	0.8899
	323	Blank	0.06179	-	1216769	-
		0.1	0.01063	82.79	0209326	0.8279
		0.3	0.00100	83.71	19692.00	0.8371
		0.5	0.00927	85.95	182544.8	0.8595
	333	Blank	0.01932	-	1561969	-
		0.1	0.00432	66.20	85069.44	0.6620
		0.3	0.00519	73.13	102201.5	0.7313
		0.5	0.00653	77.63	128588.8	0.7763
CQBP	303	Blank	0.01701	-	334960.9	-
		0.1	0.00169	90.37	33279.48	0.9037
		0.3	0.00101	94.30	19888.92	0.9430
		0.5	0.00064	96.23	12602.88	0.9623
	313	Blank	0.04465	-	879247.8	-
		0.1	0.00496	88.89	97672.32	0.8889
		0.3	0.00379	91.51	74632.68	0.9151
		0.5	0.00310	93.05	61045.20	0.9305
	323	Blank	0.06613	-	13022.32	-
		0.1	0.01098	83.39	216218.2	0.8339
		0.3	0.00861	86.98	169548.1	0.8698
		0.5	0.00686	89.62	135087.1	0.8962
	333	Blank	0.08613	-	16960.72	-
		0.1	0.01652	79.78	325311.8	0.7978
		0.3	0.01258	80.81	247725.4	0.8081
		0.5	0.01198	86.09	235910.2	0.8609

Table-3
Activation energy (E_a) and free energy ($\Delta G^{°}_{ads}$) for the corrosion of mild steel in 1 M HCl at different concentration of the inhibitors

Name of the inhibitor	Concentration (mM)	Activation energy (E_a) KJ	Gibb's free energy ($\Delta G^{°}_{ads}$) at various temperature KJ/mol			
			303	313	323	333
CQEP	Blank	53.71	-	-	-	-
	0.1	38.68	-26.82	-26.02	-25.65	-23.38
	0.3	23.28	-27.16	-26.44	-25.81	-24.21
	0.5	20.12	-27.86	-26.96	-26.25	-24.83
CQBP	Blank	53.71	-	-	-	-
	0.1	32.53	-27.33	-26.93	-25.76	-25.15
	0.3	29.92	-28.76	-27.68	-26.48	-25.31
	0.5	27.42	-29.85	-28.23	-27.12	-26.28

A. Ilamparithi, et.al.[9] was reported that the inhibition efficiency increases with increase in the alkyl substituent in piperidin-4-one compounds. Similarly, in our present study, more alkyl groups are present in the 3-butyl-2,6-biquinonyl-piperidin-4-one (CQBP) and also it have been more carbocation. So that the inhibition efficiency increases (CQBP) rather than the 3-ethyl-2,6-biquinonyl-piperidin-4-one (CQEP).

Effect of temperature: The effect of temperature on the corrosion of mild steel in 1 M HCl solution in absence and presence of 3-ethyl-2,6-biquinonyl-piperidin-4-one (CQEP) and 3-butyl-2,6-biquinonyl-piperidin-4-one (CQBP) were studied at different temperatures (303-333 K) by weight loss measurements. This effect of temperature on the inhibited acid-metal reaction is very complex because many changes occur on the metal surface such as rapid etching, desorption of inhibitor and the inhibitor itself may undergo decomposion. The data of table 2 shows that the inhibition efficiency decreases with rise in temperature. This may be probably due to increased rate of desorption of CQEP and CQBP inhibitor from the mild steel surface at higher temperature.

Arrhenius plots for the corrosion rates of mild steel with and without inhibitor for various concentrations (0. 1, 0. 3 and 0. 5 mM) are shown in figure-4. From this figure-4 depicts the plot of log CR vs. 1000/T and the values of activation energy (E_a) obtained from the slope. The higher value of activation energy (E_a) in the presence of the inhibitor than in its absence is attributed to its physical adsorption and its chemical adsorption

is in the opposite case.

In the present study the lower value of E_a for mild steel in presence of both inhibitor (CQEP and CQBP) compared to that in its absence of the inhibitor is attributed to its chemical adsorption is presented in table-3.

The experimental corrosion rate values obtained from the weight loss measurements in 1M HCl in the presence and absence of inhibitors was used to calculate the change in enthalpy (ΔH°) and entropy (ΔS°) of activation using the transition state plot and shown in figure-5 . A plot of log (Corrosion rate/T) Vs 1000/T gave a straight line with a slope of $(-\Delta H^\circ/2.303R)$ and an intercept of $[\log (R/Nh) + \Delta S^\circ / 2.303R]$ from which the values of ΔS° and ΔH° were calculated and tabulated-4.

Table-4
Thermodynamic parameters for different concentrations of mild steel corrosion in 1 M HCl

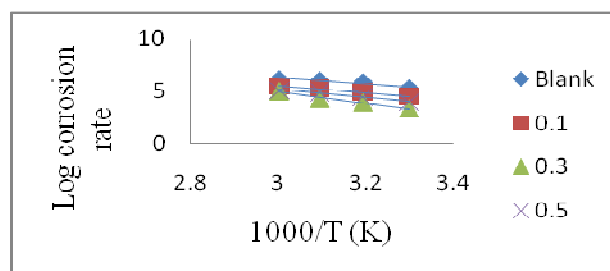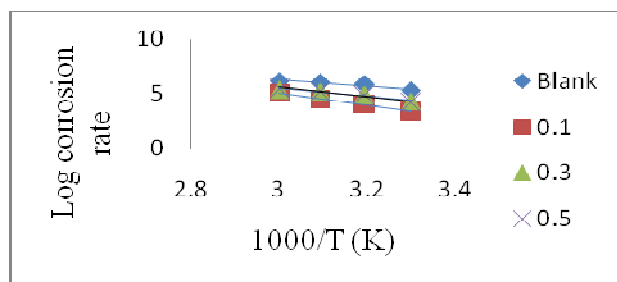| Name of the inhibitor	Concentration (mM)	Mild steel	
		ΔH^0 KJ/mole	ΔS^0 KJ/mole
CQEP	Blank	55.77	28.92
	0.1	21.32	17.65
	0.3	34.02	22.18
	0.5	51.06	29.36
CQBP	0.1	61.73	31.18
	0.3	68.19	32.96
	0.5	78.26	35.93

Figure-4
Arrhenius plot of corrosion of mild steel in 1 M HCl solution in the absence and presence of different concentrations of the CQEP and CQBP
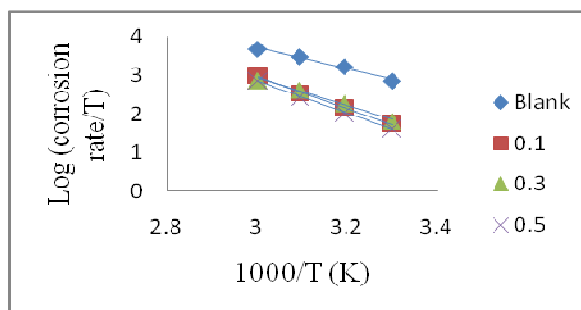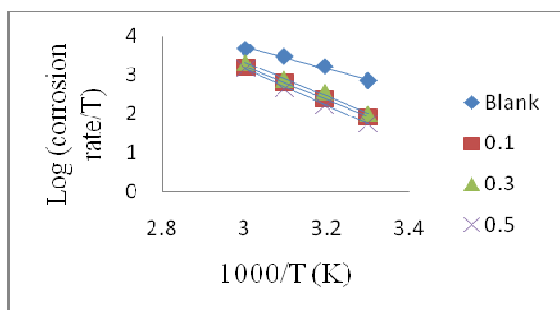

Figure-5
Transition plot of corrosion of mild steel in 1M HCl solution in the absence and presence of different concentrations of the CQEP and CQBP

The $\Delta H^{°}$ values for mild steel in presence of inhibitor (CQEP: 51.06 KJ/mol and CQBP : 78.26 KJ/mol) and absence of inhibitor 55.77 KJ/mol. The results showed that the lower values in the presence of inhibitor (CQEP and CQBP) as compared with absence of the inhibitor, indicates chemical adsorption of the inhibitor on the metal surface and also positive for enthalpy of activation $\Delta H^{°}$ reflecting the endothermic nature of the corrosion process.

The $\Delta S^{°}$ values for mild steel in presence of inhibitor (CQEP: 29.36 KJ/mol and CQBP: 35.93 KJ/mol) and absence of inhibitor (28.36 KJ/mol). The above results concluded that the entropy of activation values are positive for presence of inhibitor (CQEP and CQBP) than that for the absence of inhibitor. This suggests that the disorderness occurred while moving from reactants to the activated complex.

Adsorption isotherm: The adsorption isotherm describes the adsorption behavior of organic compounds in order to know the adsorption mechanism. The most frequently used adsorption isotherms are Langmuir, Tempkin, Frumkin and Freundlich. The primary step in the action of inhibitors in acid solution is generally agreed to be the adsorption on the metal surface. This involves the assumption that the corrosion reactions are prevented from occurring over the area (or active sites) of the metal surface covered by adsorbed inhibitor species, whereas these corrosion reactions occur normally on the inhibitor-free area. Accordingly, the fraction of surface covered with inhibitor species (Θ =IE%/100) can follow as a function of inhibitor concentration and solution temperature. The surface coverage (Θ) data are very useful on discussing the adsorption characteristics. When the fraction of surface covered is determined as a function of the concentration at constant temperature, adsorption isotherm could be evaluated at equilibrium condition. The dependence of the fraction of the surface covered Θ on the concentration C of the inhibitor was tested graphically by fitting it to Langmuir's isotherm, which assumes that the solid surface contains a fixed number of adsorption sites and each site holds one adsorbed species figure-6 shows the linear plots for C/ Θ versus C, suggesting that the adsorption obeys the Langmuir's isotherm:

$$C/\Theta = 1/K + C$$

Where 'K' is the equilibrium constant of adsorption.

The R^2 values obtained from the plots are very close to unity. This is because the interaction between the adsorbed species on the metal surface and those between the adsorbed organic molecules on the anodic and cathodic sites of the metal play important role in this process.

Free energy of the adsorption ($\Delta G°_{ads}$) calculated using
$$\Delta G°_{ads} = - RT \ln (55.5K)$$

Where, 55.5 are the concentration of water in solution expressed in molar, R is the gas constant, and T the absolute temperature. The negative values of $\Delta G°_{ads}$ are constituent with the spontaneity of the adsorption process and the stability of the adsorbed layer on the mild steel surface. Generally, values of $\Delta G°_{ads}$ up to -40 KJ/mol are consistent with electrostatic interaction between the charged molecules and the charged metal (physisorption), while those more negative than -40 KJ/mol involve charge sharing or transfer of electrons from the organic molecules to the metal surface to form a coordinate type of bond which indicates chemisorptions. Therefore, for the present work the value of $\Delta G°_{ads}$ is shown in the table 3 it has been slightly higher than -20 KJ/mol and not more than -40 KJ/mol (mild steel: CQBP -29.85 KJ/mol to -26.28 KJ/mol. So that it indicates the adsorption of both the inhibitors are chemical adsorptions on the mild steel.

Electrochemical measurements: Polarization studies: Polarization curves for mild steel in 1 M HCl without and with addition of different concentrations (0.1, 0.3 nd 0.5 mM) of the inhibitor (CQEP and CQBP) are shown in figure-7. The values of electrochemical parameters associated with polarization measurements, such as corrosion potential (E_{corr}), corrosion current density (I_{corr}), Tafel slopes (b_a ,b_c) and calculated inhibition efficiency (IE%) are listed in table-5.
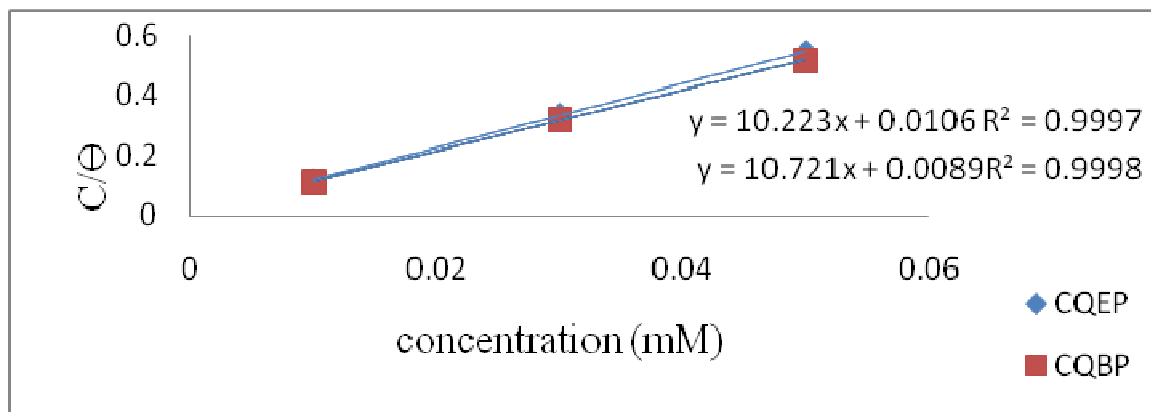

Figure-6
Langmuir plot for mild steel of inhibitor in 1 M HCl at room temperature

Table-5
Potentiodynamic polarization parameters for the corrosion of mild steel in
1 M HCl with and without inhibitor

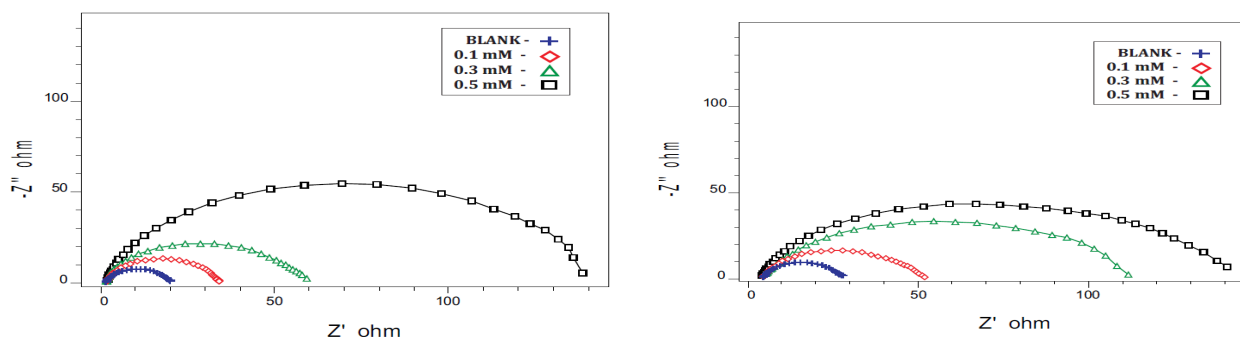| Name of the inhibitor	Inhibitor concentration (mM)	I_{corr} ($\mu A/cm^2$) x10^{-4}	E_{corr} (mV vs SCE)	b_c (mV/dec)	b_a (mV/dec)	Inhibition efficiency (%)
CQEP	Blank	8.50	-0.5427	0.118	0.094	-
	0. 1	1.43	-0.4917	0.134	0.070	83.10
	0.3	0.66	-0.4933	0.107	0.093	90.27
	0.5	0.77	-0.4880	0.109	0.089	92.23
CQBP	0.1	1.80	-0.5080	0.129	0.069	78.81
	0.3	0.57	-0.5022	0.103	0.080	91.93
	0.5	0.68	-0.4867	0.113	0.084	93.24

Figure-7
Polarization curves for mild steel in 1M HCl for CQEP and CQBP inhibitor

In the present study, the corrosion potential (E_{corr}) values slightly shifted toward both positive and negative direction in the presence of various concentrations (0.1, 0.3 and 0.5 mM) of the inhibitors (CQEP and CQBP) in 1 M HCl solution, indicating both inhibitors (CQEP and CQBP) acted as a mixed type inhibitors. However, it is clearly observed from figure-6, indicating that the addition of inhibitor molecule reduces both anodic dissolution and cathodic reduction.

In addition, from the table-5, the slope of the cathodic Tafel lines (b_c) and anodic Tafel lines (b_a) are observed to slightly change by the addition of the inhibitors (CQEP and CQBP), which indicates the influence of the inhibitors (CQEP and CQBP) on the cathodic and anodic reactions, but the cathodic curves are more affected. From the table-5 apparently showed that, Corrosion current density I_{corr} (mild steel: 8.50-0.68 ($\mu A/cm^2$ x10^{-4}) decreased with increasing the inhibitor concentrations and the inhibition efficiencies increased. Based on this observation it can be concluded that the inhibitors are mixed type.

Atomic absorption Spectroscopic studies (AAS): Atomic absorption spectroscopic method measures the concentration of ions in the solution. The percentage inhibition efficiency of the inhibitor (CQEP and CQBP) towards the dissolution of iron was calculated by measuring the dissolved iron in the corroding solution with and without inhibitor. The results are presented in the table-7 which shows that increase in concentration (0.5 mM) of inhibitor decreases the amount of dissolved iron resulting in increased inhibition efficiency. The percentage inhibition efficiency obtained by this technique was found to be in good agreement with that obtained from the conventional method.

Electrochemical Impedance spectroscopy: Impedance spectra (Nyquist plots) of mild steel in 1 M HCl containing various concentrations (0.1, 0.3 and 0.5 mM) of the inhibitor at 30°C are shown in figure-8. Nyquist plots contain depressed semicircles with the centre under the real axis. The size of the semicircle increases with the inhibitor concentration, indicating the charge transfer process as the main controlling factor of the corrosion of mild steel. It is apparent from the plots that the impedance of the inhibited solution has increased with the increase in concentration of the inhibitor. The experimental results of EIS measurements for the corrosion of mild steel in 1 M HCl in the absence and presence of inhibitor are given in table-6. It can be concluded that Charge transfer resistance (R_t) value increased with increase in the concentration of the inhibitor, whereas values of the double layer capacitance (C_{dl}) of the interface start decreasing, with increase in inhibitor concentration, which is most probably due to the decrease in local dielectric constant and/or increase in thickness of the electrical double layer.

Table-6
Impendence polarization parameters for the corrosion of mild steel in 1 M HCl with and without inhibitor

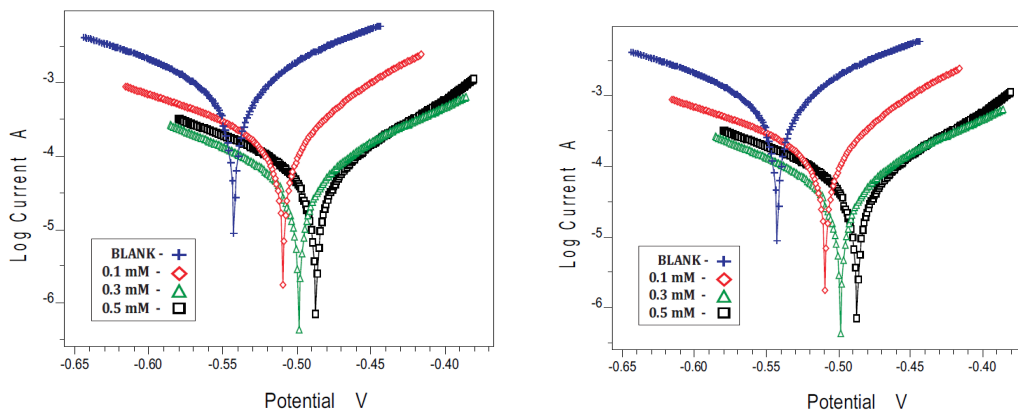| Name of the inhibitor	Inhibitor concentration (mM)	R_t (ohms)	C_{dl} (farads x10^5)	Inhibition efficiency (%)
CQEP	Blank	15.72	3.91	-
	0.1	58.00	2.19	72.89
	0.3	88.16	2.01	82.16
	0.5	92.70	1.50	83.04
CQBP	0.1	53.63	3.31	53.25
	0.3	75.50	2.16	79.17
	0.5	101.0	2.10	84.43

Figure-8
Nyquist diagram for mild steel in 1M HCl for CQEP and CQBP inhibitor

Table-7
Amount of dissolved mild steel present in the corrosive solution with and without inhibitors in 1 M HCl measured using AASS.No

Name of the inhibitor	Inhibitor concentration (mM)	Amount of mild steel in corrodant (mg/l)	Inhibition efficiency (%)
CQEP	Blank	26.40	-
	0.5	4.146	84.29
CQBP	0.5	2.356	91.07

Surface morphology: SEM photograph of the mild steel samples in the presence and absence of inhibitor CQBP are shown in figure-9. Close examination of the SEM image revealed that the specimens immersed in the inhibitor solutions are in better conditions with smooth surfaces compared with those of corroded rough and coarse uneven surfaces of mild steel immersed in 1M HCl for 3 hours. This observation indicated that corrosion rate is reduced by the adsorption of inhibitor molecule on the metal surface which act as a protective layer. The sample without inhibitor showed pits, but in presence of inhibitor the pits was minimized. The adsorption of the inhibitor (CQBP) on the metal surface was confirmed.
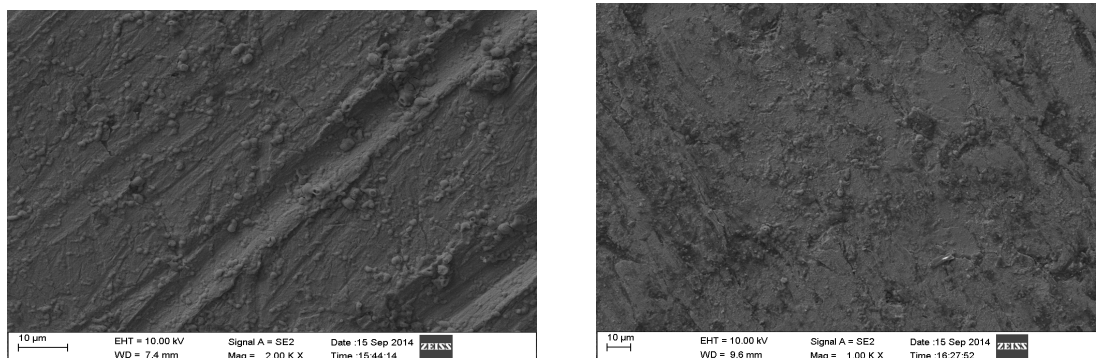

Figure-9
SEM photograph for mild steel dipped in 1 M HCl mild steel dipped in 1 M HCl with CQBP

Quantum studies: Full geometry optimizations (figure-10) of the two molecules under study (CQEP and CQBP) were performed using DFT based on Beck's three parameter exchange functional and Lee–Yang–Parr nonlocal correlation functional (B3LYP) and the 6-31G* orbital basis sets for all atoms as implemented in Gaussian 03 program. This approach has been proved to be a very powerful tool for studying corrosion inhibition Mechanism.

The quantum chemical parameters such as the energies of highest occupied molecular orbital (E_{HOMO}) and the lowest unoccupied molecular orbital (E_{LUMO}), the energy gap (ΔE) between E_{HOMO} and E_{LUMO}, dipole moment (μ), ionization potential (I), electron affinity (A), absolute electronegativity (χ), global hardness (η), global electrophilicity index (ω) and softness (S) were calculated for inhibitors (CQEP and CQBP) and gathered in table-8.

table-8 shows that the E_{HOMO} of inhibitors CQBP and CQEP are almost the same: - 6.452686 (eV) and - 6.451054 (eV) respectively. More carbocation present in the CQBP and hence transport process occurs through the inhibitor and metal surface to form a layer as compared to the CQEP inhibitor. The shape of the HOMO and LUMO is structural dependant as shown in figure-11. The inhibitor CQBP having low value of E_{LUMO} - 1.87705 eV compared to the CQEP – 1.87814 eV could have better performance as corrosion inhibitor. Because of more carbocation present in the CQBP and it have higher the tendency to accept electrons as compared to the CQEP inhibitor. The inhibitor CQBP has the lowest energy gap ΔE = 4.57291 eV compared to CQEP 4.57563 eV, this means that the reactivity of the CQBP inhibitor increase leading to increase the

inhibition efficiency than the CQEP. Because the number of alkyl group in the CQBP is higher than the CQEP inhibitor. The value 4.1858 (Debye) of CQBP shows better inhibition efficiency as compared to the CQEP 4.0516 (Debye). Because CQBP have high μ (Debye) value and increase the adsorption between CQBP inhibitor and metal surface. The order of electronegativity as CQBP > CQEP. The CQBP inhibitor (4.164871) have higher the value of electronegativity than the CQEP inhibitor (4.164599). The global electrphlicity index ω shows the ability of the inhibitor molecule to accept electrons. The inhibitor CQBP (3.831459) with high electrophilicity index value than the CQEP (3.587585) compound is the strongest nucleophile and therefore has the highest inhibition efficiency. The CQBP inhibitor have ability to accept electrons because of more carbocation than CQEP inhibitor.

Table-8
Calculated quantum chemical parameters of the studied molecules

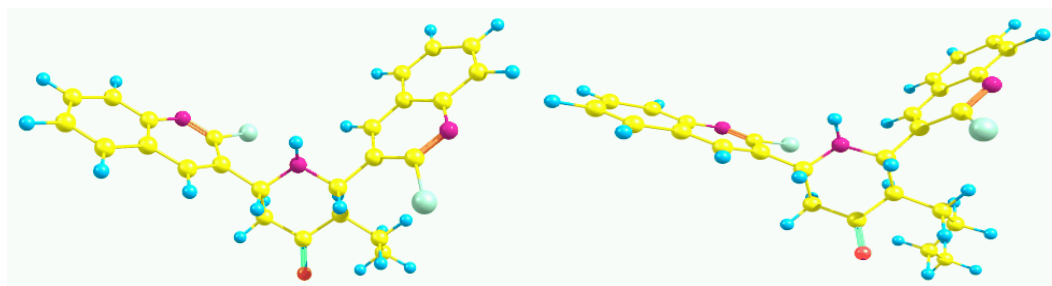| Parameters	CQEP	CQBP
E_{HOMO}	- 6.45268	- 6.45105
E_{LUMO}	- 1.87814	- 1.87705
ΔE- Energy gap	4.575630	4.572910
I- Ionization potential	6.452686	6.451054
A- Electron affinity	1.877056	1.878144
X- Electronegativity	4.164599	4.164871
η - global hardness	2.287815	2.286455
S- Softness	0.437098	0.437358
μ-Dipole moment	4.051600	4.185800
ω - Global electrophilicity	3.587585	3.831459

Figure-10
Optimized structures of the compounds CQEP and CQBP as calculated at the B3LYP/6-31G*level
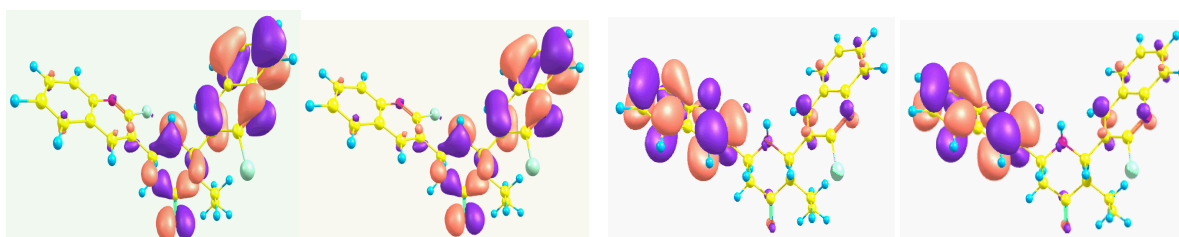**CQEP** **CQBP**

Figure-11
Schematic representation of HOMO and LUMO molecular orbital of studied molecules
CQEP-HOMO **CQBP-HOMO** **CQEP-LUMO** **CQBP-LUMO**

Conclusion

The two synthesized compounds namely, piperidin-4-one derivatives namely 3-ethyl-2,6-biquinonyl-piperidin-4-one (CQEP) and 3-butyl-2,6-biquinonyl-piperidin-4-one (CQBP).

The maximum inhibition efficiency of CQBP inhibitor in mild steel is found to be 96.23 % at 0.5 mM concentration from weight loss studies at room temperature. In mild steel the inhibition efficiency increase with respect to the concentration of the inhibitor and decreases with rise in temperature from 303 to 333 K. The decrease in the energy of activation values indicates that the addition of inhibitor (CQEP and CQBP) into the mild steel attributed to chemical adsorption.The positive values of enthalpy of activation and entropy of activation reflecting the endothermic nature, disorderness of reaction and chemical adsorption of the inhibitor on to the mild steel surface. The negative values of free energy of adsorption indicate spontaneous adsorption of the inhibitor (CQEP and CQBP) molecules on the metal surface. Electrochemical impedance spectroscopy measurement shows that increase in the inhibitor concentration causes an increase in the charge transfer resistance R_{ct} and decrease in C_{dl} value, due to the increase thickness of the adsorbed layer. Potentiodynamic polarization curves indicate that all the inhibitors behave as mixed type inhibitors but cathodic effect is more pronounced. The inhibition efficiency obtained from atomic absorption spectrophotometric studies was found to be in good agreement with that obtained from the conventional weight loss method. SEM analysis results supported the formation of a film on the mild steel. From experimental and theoretical data, the trend for the variation of the inhibition efficiencies of the compounds are CQBP > CQEP. Therefore, the use of quantum chemical parameter is appropriate in modeling the inhibitory of the studied piperidin-4-one based molecules.

Reference

1. El Adnani Z, Mcharfi M, Sfaira M, Benjelloun AT, benzakour M, Ebn Touhami M, Hammouti B and Taleb M, *Int. J. Electrochem. Sci.,***7,** 3982–3996 (**2012**)

2. Gopi D, Govindaraju KM, Prakash VCA, Manivannan V and Kavitha L, *J. Appl. Electro chem.,* **39,** 269-276 **(2009)**

3. Martinez S and Stagljar I, *J.Mol.Struct (Theochem),* **640,** 167-174 **(2003)**

4. Fouda AS., Al-Sarawy AA. and El- Katori EE, *Desalination,* **201,** 1-13 **(2006)**

5. Badr GE, Corros. Sci., **51,** 2529-2536 **(2009)**

6. Laarej K, Bouachrine M, Radi S, Kertit S and Hammouti B, *E-J. Chem.,* **7,** 419- 424 **(2010)**

7. Obot IB and Obi-Egbedi NO, *Surface Review and Letters,* **15(6),** 903-910, **(2008)**

8. Abd El-Rehim SS, Ibrahim MAM and Khaled FFJ, *Appl. Electrochem.,* **29,** 593-599 **(1999)**

9. Ilamparithi A, Ponnuamy S and Selvaraj A., *International Journal of Applied and Natural Sciences,* **3(2),** 63-80 **(2014)**